

Research Article

Piecewise Bivariate Hermite Interpolations for Large Sets of Scattered Data

Renzhong Feng^{1,2} and Yanan Zhang^{1,2}

¹ School of Mathematics and Systematic Science, Beijing University of Aeronautics and Astronautics, Beijing 100191, China

² Key Laboratory of Mathematics, Informatics and Behavioral Semantics, Ministry of Education, Beijing 100191, China

Correspondence should be addressed to Renzhong Feng; fengrz@buaa.edu.cn

Received 12 January 2013; Accepted 13 March 2013

Academic Editor: Ray K. L. Su

Copyright © 2013 R. Feng and Y. Zhang. This is an open access article distributed under the Creative Commons Attribution License, which permits unrestricted use, distribution, and reproduction in any medium, provided the original work is properly cited.

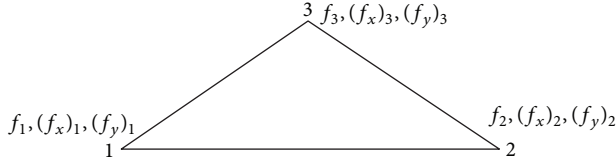
The requirements for interpolation of scattered data are high accuracy and high efficiency. In this paper, a piecewise bivariate Hermite interpolant satisfying these requirements is proposed. We firstly construct a triangulation mesh using the given scattered point set. Based on this mesh, the computational point (x, y) is divided into two types: interior point and exterior point. The value of Hermite interpolation polynomial on a triangle will be used as the approximate value if point (x, y) is an interior point, while the value of a Hermite interpolation function with the form of weighted combination will be used if it is an exterior point. Hermite interpolation needs the first-order derivatives of the interpolated function which is not directly given in scattered data, so this paper also gives the approximate derivative at every scattered point using local radial basis function interpolation. And numerical tests indicate that the proposed piecewise bivariate Hermite interpolations are economic and have good approximation capacity.

1. Introduction

The approximation to higher dimensional scattered data is one of the hot and difficult problems in approximation theory field. Due to the characteristics of scattered data, such as the large amount, irregularity, and high dimensionality, it is difficult to construct the approximation methods for them. However, the approximation method to scattered data has been widely applied in many fields, that is, estimating the parameter of input nonlinear system [1–3], solving partial differential equations, surface reconstruction in reverse engineering, data visualization, and so on. The most frequently-used approximation methods include interpolation by spline, interpolation by radial basis function, and the least square approximation. The interpolations by spline have two types, which are global interpolation and local interpolation, respectively. The global spline interpolation [4] is not able to deal with large scale of scattered data, while the local spline interpolation [5–7] needs smooth joining between piece and piece. The radial basis function interpolation [8, 9] requires solving a large scale of linear

system, and the least square approximation [10, 11] also requires solving a certain scale of linear system. This is a problem that does not easily work out in the computation. It is well known that Hermite interpolation has higher approximation accuracy than interpolation that only interpolates function values. This is because it interpolates not only the function value, but also the derivative value. However, how to construct multivariate Hermite interpolation for large sets of scattered data is an important research consideration which is also a difficult task. At present, some results have been published [12–14]; however, these methods all require solving a certain scale of linear system. Therefore, they are not suitable for approximating to large scale of scattered data.

This paper proposes two piecewise bivariate Hermite interpolation methods for large sets of scattered data. One of them uses exact derivative in Hermite interpolation, and the other one does the approximate derivative. Both methods are economic, free us from solving any linear systems, and have better approximation capacity. Therefore, they are especially suitable for the approximation to large

FIGURE 1: Interpolation triangle T_{123} .

sets of scattered data. These interpolation methods firstly use Delaunay triangulation method [15] to make a triangulation mesh based on the given scattered point set and then divide the computational point (x, y) into two types of interior point and exterior outer point. If point (x, y) is an interior point, then the value of the Hermite interpolation function on the triangle which point (x, y) lies on is regarded as the approximate value of the approximated function, while if point (x, y) is an exterior point, then the value of a Hermite interpolation with a form of weighted combination is regarded as the approximate value. Hermite interpolation needs the first-order derivatives of the interpolated function; however, the derivative information is not directly given at scattered data, so this paper gives the approximate derivative at every scattered point by using local radial basis function interpolation.

The structure of this paper is organised as follows. The Hermite interpolation on triangle is presented in Section 2. The construction of piecewise bivariate Hermite interpolation is presented in Section 3. The estimation of partial derivative at every scattered point by local radial basis function interpolation is presented in Section 4. Some numerical tests and comparisons between constructed schemes and other interpolation schemes in accuracy and efficiency are carried out in Section 5. This paper ends with a section of brief conclusion.

2. Hermite Interpolation Based on Triangle

Given the values and partial derivatives of a bivariate function $f(x, y)$ at three vertices (x_i, y_i) , $i = 1, 2, 3$ of a triangle T_{123} (their vertices 1, 2, 3 are arranged counter to clockwise), that is, $f_i, (f_x)_i, (f_y)_i$, $i = 1, 2, 3$ (see Figure 1). A bivariate Hermite interpolation polynomial $H_{123}(x, y)$ is to be constructed satisfying the following interpolation conditions:

$$\begin{aligned} H_{123}(x_i, y_i) &= f_i, & \frac{\partial H_{123}}{\partial x}(x_i, y_i) &= (f_x)_i, \\ \frac{\partial H_{123}}{\partial y}(x_i, y_i) &= (f_y)_i, & i &= 1, 2, 3. \end{aligned} \quad (1)$$

In order to infer the expression of Hermite interpolation from interpolation conditions (1), the barycenter coordinate of a triangle needs to be introduced first. It is assumed that $P(x, y)$ is a point on triangle T_{123} and its barycentric

coordinates is denoted as (l_1, l_2, l_3) . Then the relation between its cartesian coordinates and barycentric coordinates is

$$\begin{aligned} l_1 &= \frac{(x_2 y_3 - x_3 y_2) + (y_2 - y_3)x + (x_3 - x_2)y}{2S}, \\ l_2 &= \frac{(x_3 y_1 - x_1 y_3) + (y_3 - y_1)x + (x_1 - x_3)y}{2S}, \\ l_3 &= \frac{(x_1 y_2 - x_2 y_1) + (y_1 - y_2)x + (x_2 - x_1)y}{2S}, \end{aligned} \quad (2)$$

$$l_1 + l_2 + l_3 = 1, \quad l_1, l_2, l_3 \geq 0,$$

$$x = x_1 l_1 + x_2 l_2 + x_3 l_3,$$

$$y = y_1 l_1 + y_2 l_2 + y_3 l_3,$$

where S is the area of the triangle T_{123} and

$$S = \begin{vmatrix} 1 & x_1 & y_1 \\ 1 & x_2 & y_2 \\ 1 & x_3 & y_3 \end{vmatrix}. \quad (3)$$

Making use of transformation (2), the interpolation conditions (1) can be changed into the following form under barycentric coordinates:

$$\begin{aligned} H_{123}(1, 0) &= f_1, & H_{123}(0, 1) &= f_2, \\ H_{123}(0, 0) &= f_3, \\ \frac{\partial H_{123}}{\partial l_1}(1, 0) &= (x_1 - x_3)(f_x)_1 + (y_1 - y_3)(f_y)_1, \\ \frac{\partial H_{123}}{\partial l_1}(0, 1) &= (x_1 - x_3)(f_x)_2 + (y_1 - y_3)(f_y)_2, \\ \frac{\partial H_{123}}{\partial l_1}(0, 0) &= (x_1 - x_3)(f_x)_3 + (y_1 - y_3)(f_y)_3, \\ \frac{\partial H_{123}}{\partial l_2}(1, 0) &= (x_2 - x_3)(f_x)_1 + (y_2 - y_3)(f_y)_1, \\ \frac{\partial H_{123}}{\partial l_2}(0, 1) &= (x_2 - x_3)(f_x)_2 + (y_2 - y_3)(f_y)_2, \\ \frac{\partial H_{123}}{\partial l_2}(0, 0) &= (x_2 - x_3)(f_x)_3 + (y_2 - y_3)(f_y)_3. \end{aligned} \quad (4)$$

A complete bivariate polynomial of three degrees $p_3(x, y) = \sum_{i+j=0}^3 c_{ij} x^i y^j$ has ten undetermined coefficients. Under barycentric coordinate its expression is

$$\begin{aligned} p_3(x, y) &= c_1 l_1^3 + c_2 l_2^3 + c_3 l_3^3 + c_4 l_1^2 l_2 + c_5 l_1^2 l_3 \\ &\quad + c_6 l_2^2 l_1 + c_7 l_2^2 l_3 + c_8 l_3^2 l_1 + c_9 l_3^2 l_2 + c_{10} l_1 l_2 l_3. \end{aligned} \quad (5)$$

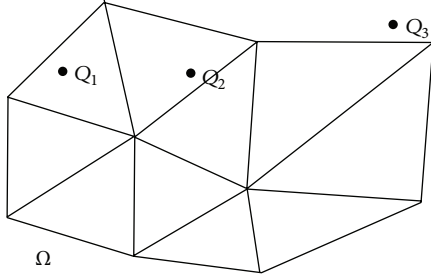


FIGURE 2: The exhibition of interior and exterior points.

Since the Hermite interpolation conditions (1) or (4) only provide 9 conditions, we construct a Hermite interpolation polynomial with nine coefficients

$$\begin{aligned} H_f(l_1, l_2) &= c_1 l_1^3 + c_2 l_2^3 + c_3 l_3^3 + c_4 l_1^2 l_2 + c_5 l_1 l_2^2 + c_6 l_2^2 l_1 \\ &\quad + c_7 l_2^2 l_3 + c_8 l_3^2 l_1 + c_9 l_3^2 l_2 + 0.5(c_7 + c_8 + c_9) l_1 l_2 l_3, \end{aligned} \quad (6)$$

which meets interpolation condition (4). Then the values of the coefficients in formula (6) can be obtained:

$$\begin{aligned} c_1 &= f_1, & c_2 &= f_2, & c_3 &= f_3, \\ c_4 &= 3f_1 - \frac{\partial H_{123}}{\partial l_1}(1, 0) + \frac{\partial H_{123}}{\partial l_2}(1, 0), \\ c_5 &= 3f_1 - \frac{\partial H_{123}}{\partial l_1}(1, 0), \\ c_6 &= 3f_2 - \frac{\partial H_{123}}{\partial l_2}(0, 1) + \frac{\partial H_{123}}{\partial l_1}(0, 1), \\ c_7 &= 3f_2 - \frac{\partial H_{123}}{\partial l_2}(0, 1), \\ c_8 &= 3f_3 + \frac{\partial H_{123}}{\partial l_1}(0, 0), \\ c_9 &= 3f_3 + \frac{\partial H_{123}}{\partial l_2}(0, 0). \end{aligned} \quad (7)$$

Combining (4), (6), and (7), the Hermite interpolation polynomial satisfying (4) can be written as

$$\begin{aligned} H_{123}(x, y) &= \sum_{i=1}^3 [\alpha_i(x, y) f_i + \beta_i(x, y) (f_x)_i + \gamma_i(x, y) (f_y)_i], \end{aligned} \quad (8)$$

where

$$\begin{aligned} \alpha_1(x, y) &= l_1^3 + 3l_2 l_1^2 + 3l_3 l_1^2 + 2l_1 l_2 l_3, \\ \alpha_2(x, y) &= l_2^3 + 3l_1 l_2^2 + 3l_3 l_2^2 + 2l_1 l_2 l_3, \\ \alpha_3(x, y) &= l_3^3 + 3l_1 l_3^2 + 3l_2 l_3^2 + 2l_1 l_2 l_3, \\ \beta_1 &= (x_2 - x_1)(l_1^2 l_2 + 0.5l_1 l_2 l_3) \\ &\quad + (x_3 - x_1)(l_1^2 l_3 + 0.5l_1 l_2 l_3), \\ \beta_2 &= (x_1 - x_2)(l_2^2 l_1 + 0.5l_1 l_2 l_3) \\ &\quad + (x_3 - x_2)(l_2^2 l_3 + 0.5l_1 l_2 l_3), \\ \beta_3 &= (x_1 - x_3)(l_3^2 l_1 + 0.5l_1 l_2 l_3) \\ &\quad + (x_2 - x_3)(l_3^2 l_2 + 0.5l_1 l_2 l_3), \\ \gamma_1 &= (y_2 - y_1)(l_1^2 l_2 + 0.5l_1 l_2 l_3) \\ &\quad + (y_3 - y_1)(l_1^2 l_3 + 0.5l_1 l_2 l_3), \\ \gamma_2 &= (y_1 - y_2)(l_2^2 l_1 + 0.5l_1 l_2 l_3) \\ &\quad + (y_3 - y_2)(l_2^2 l_3 + 0.5l_1 l_2 l_3), \\ \gamma_3 &= (y_1 - y_3)(l_3^2 l_1 + 0.5l_1 l_2 l_3) \\ &\quad + (y_2 - y_3)(l_3^2 l_2 + 0.5l_1 l_2 l_3). \end{aligned} \quad (9)$$

3. Bivariate Piecewise Hermite Interpolation for Large Sets of Scattered Data

Given a set of scattered data $\{(x_j, y_j, f_j)\}_{j=1}^N \subset R^3$, which are assumed to be sampled from a function $f(x, y), (x, y) \in \Omega$. The partial derivatives of $f(x, y)$ at the set of points $\{(x_j, y_j)\}_{j=1}^N \subset \Omega \subset R^2$ are given as $(f_x)_j, (f_y)_j, j = 1, \dots, N$. Taking the N scattered points as nodes, a triangulation mesh, T , is constructed in domain Ω using Delaunay triangulation method. If point $(x, y) \in \Omega \subset R^2$ lies on a triangle of T , it is called as an interior point, otherwise, an exterior point. For example, points Q_1, Q_2 in Figure 2 are interior points, while point Q_3 is an exterior point. Next we will give the approximate value $Q_f(x, y)$ of $f(x, y)$ according to the category of point (x, y) .

3.1. Interior Point. Suppose that point (x, y) lies on a triangle $T_{jkl} \subset T$ whose vertices are $(x_j, y_j), (x_k, y_k), (x_l, y_l)$. We now

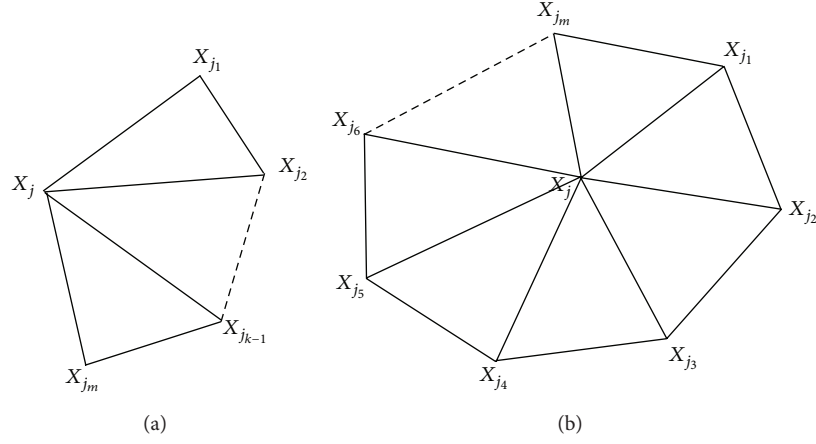


FIGURE 3: The local radial basis interpolation point set A_j around point X_j , (a) X_j is a boundary point of T and (b) X_j is an interior node point of T .

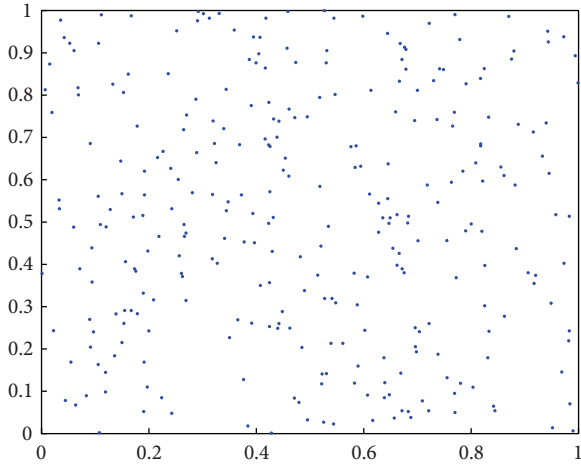


FIGURE 4: 300 scattered points randomly selected in $[0, 1] \times [0, 1]$.

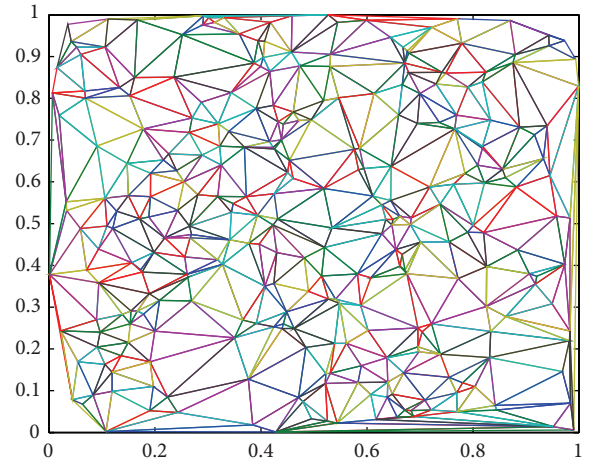


FIGURE 5: Delaunay triangulation based on Figure 4.

construct a Hermite interpolation polynomial as (8) on triangle T_{jkl} satisfying the following conditions:

$$\begin{aligned}
 H_{jkl}(x_j, y_j) &= f_j, & \frac{\partial H_{jkl}}{\partial x}(x_j, y_j) &= (f_x)_j, \\
 \frac{\partial H_{jkl}}{\partial y}(x_j, y_j) &= (f_y)_j, & H_{jkl}(x_k, y_k) &= f_k, \\
 \frac{\partial H_{jkl}}{\partial x}(x_k, y_k) &= (f_x)_k, & \frac{\partial H_{jkl}}{\partial y}(x_k, y_k) &= (f_y)_k, \\
 H_{jkl}(x_l, y_l) &= f_l, & \frac{\partial H_{jkl}}{\partial x}(x_l, y_l) &= (f_x)_l, \\
 \frac{\partial H_{jkl}}{\partial y}(x_l, y_l) &= (f_y)_l.
 \end{aligned}
 \tag{10}$$

Then let $Q_f(x, y) = H_{jkl}(x, y)$, so that $Q_f(x, y) \approx f(x, y)$.

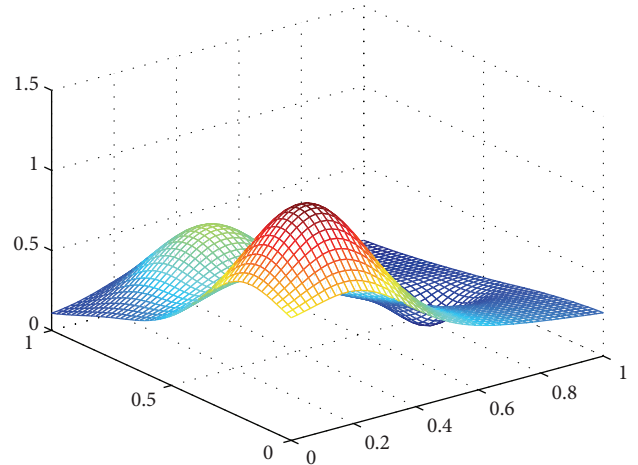


FIGURE 6: The graph of Franke function.

3.2. Exterior Point. When point (x, y) does not belong to any triangle within T , we construct the following form of Hermite interpolation:

$$Q_f(x, y) = \sum_{j=1}^N W_j(x, y) H_{f,j}(x, y), \quad (11)$$

satisfying interpolation conditions

$$\begin{aligned} Q_f(x_j, y_j) &= f_j, & \frac{\partial Q_f}{\partial x}(x_j, y_j) &= (f_x)_j, \\ \frac{\partial Q_f}{\partial y}(x_j, y_j) &= (f_y)_j, & j &= 1, 2, \dots, N. \end{aligned} \quad (12)$$

In this paper, we take $H_{f,j}(x, y)$ as a Hermite interpolation polynomial with the same form of (8) on triangle T_{jkl} with the least area among all triangles with vertex (x_j, y_j) , satisfying interpolation conditions (10). $H_{f,j}(x, y)$ is called as node basis function and function $W_j(x, y)$ is called as weighted function. In order to satisfy interpolation conditions (12), these weighted functions are required for satisfying conditions

$$W_j(x_i, y_i) = \delta_{ij}, \quad i, j = 1, \dots, N, \quad (13)$$

$$\sum_{j=1}^N W_j(x, y) \equiv 1, \quad W_j(x, y) \geq 0, \quad j = 1, \dots, N, \quad (14)$$

$$\frac{\partial W_j}{\partial x}(x_i, y_i) = \frac{\partial W_j}{\partial y}(x_i, y_i) = 0, \quad i, j = 1, \dots, N. \quad (15)$$

In the paper we take the weighted functions in (11) as those in the literature [16]:

$$W_j(x, y) = \frac{(1/\rho_j^2)}{\sum_{k=1}^N (1/\rho_k^2)}, \quad (16)$$

where

$$\begin{aligned} \frac{1}{\rho_k} &= \frac{(R_k - d_k)_+}{R_k d_k}, \\ (R_k - d_k)_+ &= \begin{cases} R_k - d_k & R_k - d_k \geq 0, \\ 0 & R_k - d_k < 0, \end{cases} \quad (17) \\ d_k &= d_k(x, y) = \sqrt{(x - x_k)^2 + (y - y_k)^2}. \end{aligned}$$

The value of R_k in (17) can be selected by user properly. It can be seen that when $(x, y) \rightarrow (x_j, y_j)$, $(1/\rho_j^2) \rightarrow +\infty$, thereby $W_j(x, y) \rightarrow 1$; when $(x, y) \rightarrow (x_k, y_k)$, $k \neq j$ and $(1/\rho_k^2) \rightarrow +\infty$, thereby $W_j(x, y) \rightarrow 0$. Thus W_j satisfies condition (13). W_j in formula (16) satisfies condition (14) obviously, and the proof of which can be found in literature [16]. If $1/\rho_j$ is determined by (17), then when $d_j(x, y) > R_j$, $W_j(x, y) = 0$. So in case of R_j being appropriately selected (R_j is also called as influence radius of node basis function), there are only several nonzero terms in sum $\sum_{k=1}^N W_k(x, y)$.

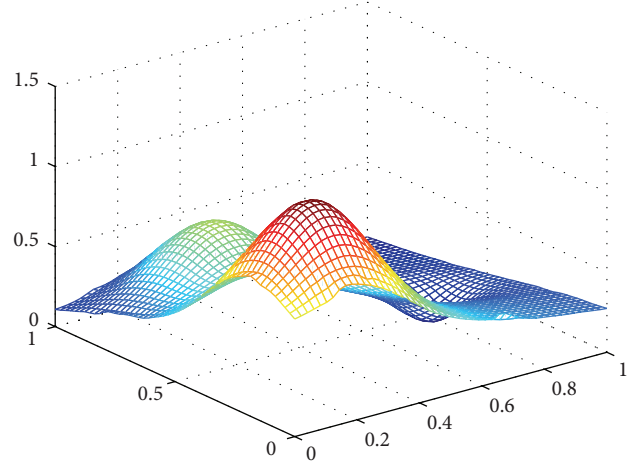


FIGURE 7: The graph of $Q_f(x, y)$ based on Figure 4.

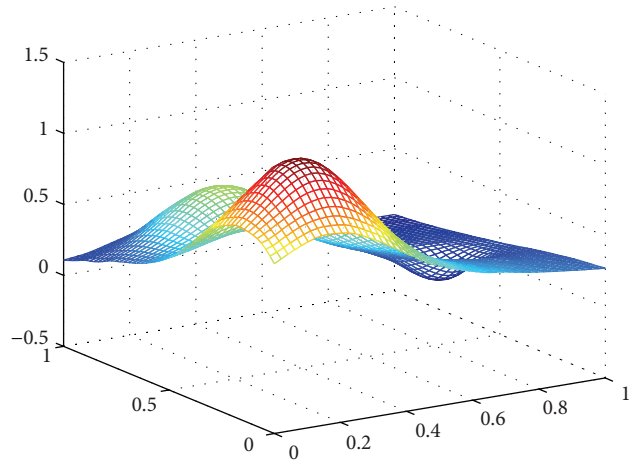


FIGURE 8: The graph of $\tilde{Q}_f(x, y)$ based on Figure 4.

Then it can be found that interpolation function (11) which takes functions (16) and (17) as its weight functions is a local Hermite interpolation. When applying (11), we can use different influence radius at every node, so we can use the same radius R . The following computational formulation of uniform influence radius R in (18) is from [16]:

$$R = \frac{D}{2} \sqrt{\frac{N_w}{N}}, \quad D = \max_{i,j} d_i(x_j, y_j). \quad (18)$$

N_w is the number of points used inside a circle of radius R .

3.3. Bivariate Piecewise Hermite Interpolation. Summing up Sections 3.1 and 3.2, a bivariate piecewise Hermite interpolation function is constructed on Ω to approximate the function $f(x, y)$

$$Q_f(x, y) = \begin{cases} H_{jkl}(x, y), & \text{if } (x, y) \in \Gamma, \\ \sum_{j=1}^N W_j(x, y) H_{f,j}(x, y), & \text{if } (x, y) \in \Omega - \Gamma, \end{cases} \quad (19)$$

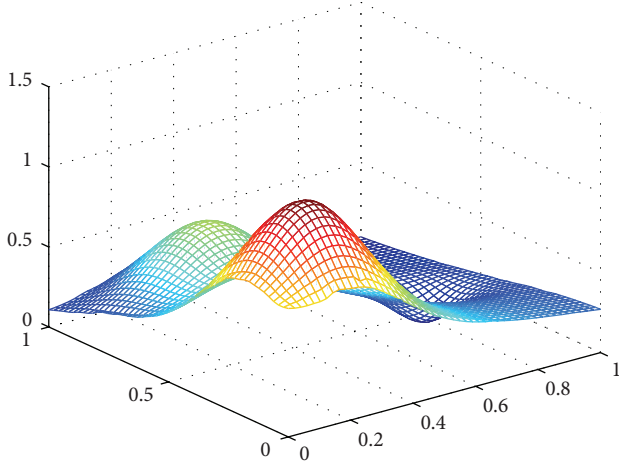


FIGURE 9: The graph of WLRBF based on Figure 4.

where T_{jkl} is a triangle within T with node (x_j, y_j) , (x_k, y_k) , (x_l, y_l) as its vertices and H_{jkl} is a Hermite interpolation polynomial on triangle T_{jkl} .

We now summarize the description of the constructed interpolation function, written as Algorithm 1.

Algorithm 1. Consider the following.

Step 1. Generate a triangle mesh T in domain Ω using Delaunay triangulation method based on given scattered point set $\{(x_j, y_j)\}_{j=1}^N \subset \Omega$.

Step 2. Judge the category of point (x, y) : interior point or exterior point.

Step 3. If point (x, y) is an interior point, then find out the triangle T_{jkl} which includes point (x, y) , compute the value of the interpolation function H_{jkl} at point (x, y) using formulas (2), (8), and (10), and take the value as the value of $Q_f(x, y)$.

Step 4. If point (x, y) is an exterior point, then compute $D = \max_{i,j} d_i(x_j, y_j)$ and select N_W to define $R = (D/2)\sqrt{N_W/N}$. The default value of N_W is set to 9, and it responds to a uniform radius. Find out the points (x_{j_l}, y_{j_l}) , $l = 1, \dots, k$ from scattered point set $\{(x_j, y_j)\}_{j=1}^N$, which belongs to the circle with radius R and center (x, y) , compute the values $W_{j_l}(x, y)$, $l = 1, \dots, k$ and $H_{f,j_l}(x, y)$, $l = 1, \dots, k$, give the sum $\sum_{l=1}^k W_{j_l}(x, y)H_{f,j_l}(x, y)$, and assign it to $Q_f(x, y)$.

4. The Estimation of Partial Derivative

In the process of using bivariate piecewise Hermite interpolation Q_f , it demands the first-order derivatives of the interpolated function $f(x, y)$ at every point, but the scattered data $\{(x_j, y_j, f_j)\}_{j=1}^N$ does not provide the derivatives. Thus we use the first-order derivative of a local radial basis interpolation to approximate the derivative of the interpolated function

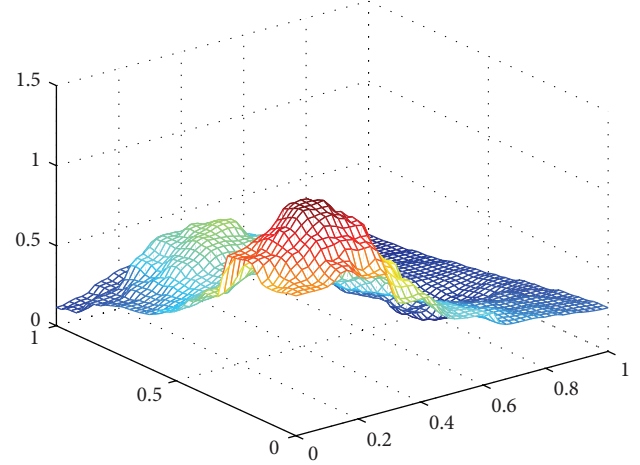
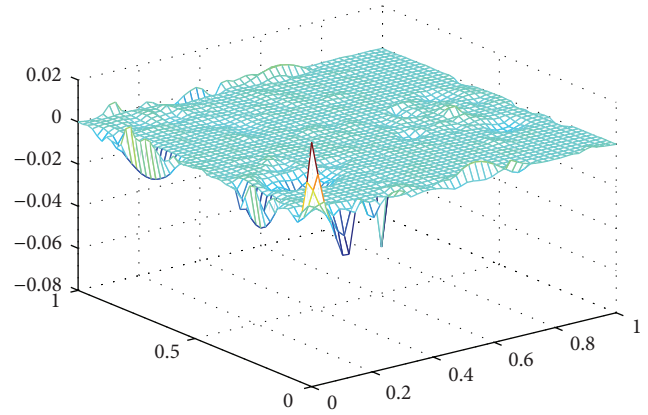


FIGURE 10: The graph of Shepard interpolation based on Figure 4.

FIGURE 11: The error graph of $Q_f(x, y)$.

$f(x, y)$ and replace this exact derivative in (19) with the approximate derivative.

The Delaunay triangulation T is a convex subdomain of Ω . Every scattered point $X_j = (x_j, y_j)$ is either a boundary point or an interior node point of T . We put the vertices of all triangles with point (x_j, y_j) as into a set, written as $A_j = (x_j, y_j) \cup \{(x_{j_l}, y_{j_l})\}_{l=1}^m$, see Figure 3.

We take the point set A_j as local radial basis function interpolation point set and multiquadric radial basis functions

$$\begin{aligned} \phi_j &= \sqrt{(x - x_j)^2 + (y - y_j)^2 + c^2}, \\ \phi_{j_1} &= \sqrt{(x - x_{j_1})^2 + (y - y_{j_1})^2 + c^2}, \\ &\vdots \\ \phi_{j_m} &= \sqrt{(x - x_{j_m})^2 + (y - y_{j_m})^2 + c^2} \end{aligned} \quad (20)$$

as local interpolation basis functions.

By solving the linear system $GC = F$,

$$G = \begin{pmatrix} \phi_j(x_j, y_j) & \phi_{j_1}(x_j, y_j) & \dots & \phi_{j_m}(x_j, y_j) \\ \phi_j(x_{j_1}, y_{j_1}) & \phi_{j_1}(x_{j_1}, y_{j_1}) & \dots & \phi_{j_m}(x_{j_1}, y_{j_1}) \\ \dots & \dots & \dots & \dots \\ \phi_j(x_{j_m}, y_{j_m}) & \phi_{j_1}(x_{j_m}, y_{j_m}) & \dots & \phi_{j_m}(x_{j_m}, y_{j_m}) \end{pmatrix},$$

$$C^T = (c_0 \ c_1 \ c_2 \ \dots \ c_m),$$

$$F^T = (f_j \ f_{j_1} \ f_{j_2} \ \dots \ f_{j_m}), \quad (21)$$

we obtained a local radial basis interpolation function $p_j(x, y) = c_0\phi_j(x, y) + c_1\phi_{j_1}(x, y) + c_2\phi_{j_2}(x, y) + \dots + c_m\phi_{j_m}(x, y)$, and then compute the first order derivatives of $p_j(x, y)$ at $X_j = (x_j, y_j)$, that is,

$$\begin{aligned} \frac{\partial p_j}{\partial x}(x_j, y_j) &= \frac{c_1(x_j - x_{j_1})}{\phi_{j_1}(x_j, y_j)} + \frac{c_2(x_j - x_{j_2})}{\phi_{j_2}(x_j, y_j)} + \dots + \frac{c_m(x_j - x_{j_m})}{\phi_{j_m}(x_j, y_j)}, \\ \frac{\partial p_j}{\partial y}(x_j, y_j) &= \frac{c_1(y_j - y_{j_1})}{\phi_{j_1}(x_j, y_j)} + \frac{c_2(y_j - y_{j_2})}{\phi_{j_2}(x_j, y_j)} + \dots + \frac{c_m(y_j - y_{j_m})}{\phi_{j_m}(x_j, y_j)}. \end{aligned} \quad (22)$$

The bivariate piecewise interpolation function Q_f using the previous approximate derivatives is written as

$$\bar{Q}_f(x, y) = \begin{cases} \bar{H}_{jkl}(x, y), & \text{if } (x, y) \in \Gamma, \\ \sum_{j=1}^N W_j(x, y) \bar{H}_{f,j}(x, y), & \text{if } (x, y) \in \Omega - \Gamma. \end{cases} \quad (23)$$

Algorithm 2 summarizes the computational process of interpolation $\bar{Q}_f(x, y)$.

Algorithm 2. Consider the following.

Step 1. Generate a triangle mesh T in Ω using Delaunay triangulation method based on the given scattered point set $\{(x_j, y_j)\}_{j=1}^N \subset \Omega$.

Step 2. Find out the local radial basis interpolation point set A_j at every point (x_j, y_j) , and compute the approximate derivatives $(\partial p_j / \partial x)(x_j, y_j)$, $(\partial p_j / \partial y)(x_j, y_j)$ at every point (x_j, y_j) using interpolation formulation (21) and (22).

Step 3. Judge the category of point (x, y) : interior point or exterior point.

Step 4. If point (x, y) is an interior point, then find out the triangle T_{jkl} which point (x, y) falls in, compute the

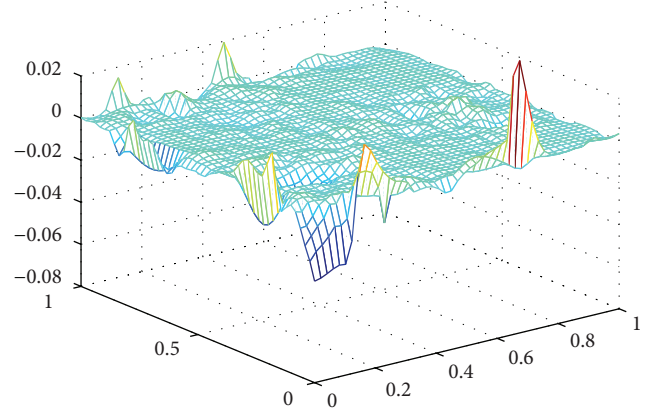


FIGURE 12: The error graph of $\bar{Q}_f(x, y)$.

value of the interpolation function H_{jkl} at point (x, y) using formulas (2), (8), and (10), and assign the value to the function $\bar{Q}_f(x, y)$.

Step 5. If point (x, y) is an exterior point, then compute $D = \max_{i,j} d_i(x_j, y_j)$ and select N_W to define $R = (D/2)\sqrt{N_W/N}$. The default value of N_W is set to 9, it responds to an uniform radius. Find out the points (x_{j_l}, y_{j_l}) , $l = 1, \dots, k$ from scattered point set $\{(x_j, y_j)\}_{j=1}^N$, which belongs to the circle with radius R and center (x, y) , compute the values $W_{j_l}(x, y)$, $l = 1, \dots, k$ and $\bar{H}_{f,j_l}(x, y)$, $l = 1, \dots, k$, give the sum $\sum_{l=1}^k W_{j_l}(x, y) \bar{H}_{f,j_l}(x, y)$, and assign it to $\bar{Q}_f(x, y)$.

5. Numerical Test

In this section, $Q_f(x, y)$ and $\bar{Q}_f(x, y)$ are used to approximate Franke function

$$\begin{aligned} f(x, y) &= 0.75 \exp\left(-\frac{(9x-2)^2 + (9y-2)^2}{4}\right) \\ &\times 0.75 \exp\left(-\frac{(9x+1)^2}{10} - \frac{(9y+1)^2}{10}\right) \\ &- 0.2 \exp\left(-(9x-4)^2 - (9y-7)^2\right) \\ &+ 0.5 \exp\left(-\frac{(9x-7)^2 + (9y-3)^2}{4}\right), \quad 0 \leq x, y \leq 1. \end{aligned} \quad (24)$$

Firstly, a scattered data set $\{(x_j, y_j, f_j)\}_{j=1}^N$ is sampled from $f(x, y)$; then, the interpolation functions $Q_f(x, y)$ and $\bar{Q}_f(x, y)$ are generated using the sampled data. Aiming at different sampled data sets, mean square error (MSE) and maximum error (MME) of the two approximate functions are computed and their approximate capacities are also

TABLE 1: The comparison of MSE and MME of $Q_f(x, y)$ and $\tilde{Q}_f(x, y)$ for the same scattered points.

Number of scatter data	N_w	Influence radius R	$Q_f(x, y) - f(x, y)$		$\tilde{Q}_f(x, y) - f(x, y)$	
			MSE	MME	MSE	MME
100	9	0.1818	$6.3064e - 005$	0.0578	$1.9664e - 004$	0.0951
300	9	0.1179	$1.2890e - 006$	0.0110	$3.8058e - 006$	0.0162
500	9	0.0918	$1.0176e - 007$	0.0030	$3.0822e - 007$	0.0043
800	9	0.0705	$2.0574e - 008$	0.0012	$1.0705e - 007$	0.0023
1000	9	0.0654	$1.2458e - 008$	0.0011	$5.2834e - 008$	0.0022

TABLE 2: The influence of influence radius on $Q_f(x, y)$ and $\tilde{Q}_f(x, y)$.

Number of scatter data	N_w	Influence radius R	$Q_f(x, y) - f(x, y)$	$\tilde{Q}_f(x, y) - f(x, y)$
			MME	MME
300	4	0.0786	0.0489	0.0906
300	9	0.1179	0.0352	0.0747
300	12	0.1361	0.0325	0.0504
300	16	0.1572	0.0307	0.0481
300	25	0.1965	0.0293	0.0447

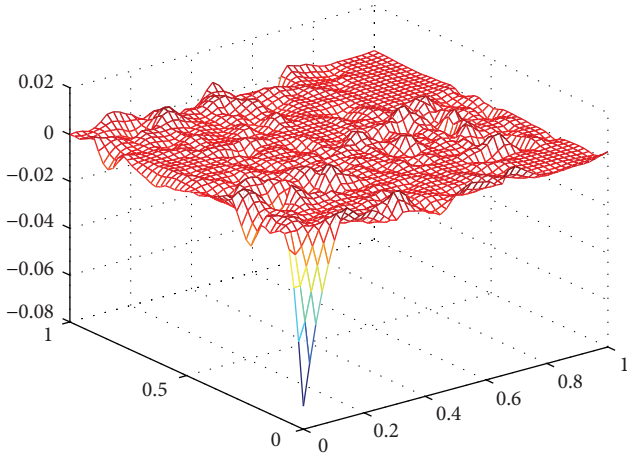


FIGURE 13: The error graph of WLRBF.

compared. Meanwhile, the approximate accuracy and computational efficiency of $Q_f(x, y)$ and $\tilde{Q}_f(x, y)$ are compared with Shepard interpolation [17] and Weighted Local RBF interpolant (abbr. WLRBF) [9]. Finally, the CPU time of these four methods is compared which are devised by MATLAB (7.12.0 R2011a) installed in a computer with Processor: Intel(R) Q8400 2.66 GHz, RAM: 4 GB. The computational results show that the methods introduced in this paper need less CPU time and have higher accuracy.

Figure 4 shows the 300 scattered points which are randomly selected from $[0, 1] \times [0, 1]$, and Figure 5 is Delaunay triangulation based on Figure 4. Figure 6 presents the graph of Franke function. Figures 7, 8, 9, and 10 describe the interpolation function graphs for the four methods of $Q_f(x, y)$, $\tilde{Q}_f(x, y)$, WLRBF, and Shepard which are also based on the 300 scattered points shown in Figure 4. It can be seen

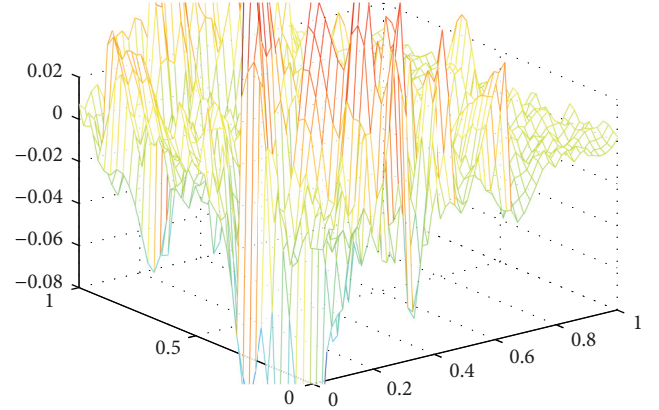


FIGURE 14: The error graph of Shepard interpolation.

that $Q_f(x, y)$, $\tilde{Q}_f(x, y)$, and WLRBF can accurately approach Franke function and are better than Shepard method. Figures 11, 12, 13, and 14 display the error graphs of the four methods based on 50×50 test points. Comparing Figure 11 with Figure 13, we can see that $Q_f(x, y)$ is much better than WLRBF method. Comparing Figures 12 and 13 for the interior points, $\tilde{Q}_f(x, y)$ is obviously better than WLRBF method. Besides, with the number of scattered data increasing, it is found that approximation capability of $\tilde{Q}_f(x, y)$ is closer to that of $Q_f(x, y)$. In case of large set of scattered points, $\tilde{Q}_f(x, y)$ can be hence absolutely superior to WLRBF.

It can be seen from Table 1 that the approximation accuracy of $Q_f(x, y)$ is higher than that of $\tilde{Q}_f(x, y)$ at the same scattered points. Meanwhile, MSE and MME of the two methods decrease with the increase of the point number. Besides, the approximating accuracies to $f(x, y)$ of $Q_f(x, y)$ and $\tilde{Q}_f(x, y)$ get closer at the same time. These results indicate that the local radial function interpolation method can be used to estimate the partial derivative when the number of data points is large enough. Therefore, $\tilde{Q}_f(x, y)$ can be used to approximate $f(x, y)$ when the partial derivative information of the scattered data is unknown.

It can be seen from Table 2 that the errors of approximation functions $Q_f(x, y)$ and $\tilde{Q}_f(x, y)$ increase with the radius of influence decreasing.

Tables 1 and 3 indicate that the approximating accuracy to $f(x, y)$ using $Q_f(x, y)$ and $\tilde{Q}_f(x, y)$ is much more accurate

TABLE 3: The comparison of MSE and MME of WLRBF method and Shepard method for the same scattered points.

Number of scatter data	N_W	Influence radius R	WLRBF		Shepard's Method	
			MSE	MME	MSE	MME
100	9	0.1818	$1.9381e-004$	0.0923	$1.9297e-003$	0.01842
300	9	0.1179	$3.6377e-006$	0.0125	$6.8555e-004$	0.1840
500	9	0.0918	$9.6671e-007$	0.0088	$4.2839e-004$	0.1967
800	9	0.0705	$2.8995e-007$	0.0046	$2.3199e-004$	0.0800
1000	9	0.0654	$1.6362e-007$	0.0033	$1.5849e-008$	0.0645

TABLE 4: The computing time of the four methods on the 50×50 grid points in the unit square.

Number of scatter data	$Q_f(x, y)$	$\tilde{Q}_f(x, y)$	WLRBF	Shepard's method
100	5.6	15.46	185.64	52.54
300	28.59	30.35	399.38	113.99
500	42.31	13.77	586.63	180.94
800	64.21	68.04	779.32	225.97
1000	80.28	80.66	1102.64	271.22

than that using WLRBF method and Shepard method with the same number of scattered points.

The data in Table 4 indicates that the computation efficiencies of $Q_f(x, y)$ and $\tilde{Q}_f(x, y)$ are much higher than those of WLRBF and Shepard methods.

6. Conclusion

In this paper, Delaunay triangulation based on planar point set is used to obtain the piecewise bivariate Hermite interpolation function in order to approximate three-dimensional scattered data sets. When point (x, y) falls on a triangle of the triangulation, the Hermite interpolation on the triangle is used for approximate calculation. If point (x, y) falls outside the triangulation area, the node basis function value weighted sum of the points that are closer to (x, y) is used as the approximate value of $f(x, y)$. Since the constructed interpolation function needs the first derivative value of the approximated function, however, the given scattered data set does not provide such information, our interpolation scheme uses local radial basis interpolation function to estimate the first derivative of each scattered point. Numerical experiments show that our methods have strong approximation ability to scattered data and the estimation of derivatives by local radial basis interpolation has high accuracy. Owing to no demand for solving linear system and the weight functions with local support, our methods are easily implemented and have high computational efficiency, so it is better than B-Spline least square fitting which needs solving a big enough linear system. The use of local radial basis function interpolation to estimate the derivatives is still consuming time. Therefore, how to construct a simple and high-accurate numerical differential formula is one of our future works. Meanwhile, for nonuniform distributed scattered data, how to more reasonably approximate them is another task in further work.

In addition, in the process of numerical experiments, we found that the triangulation based on scattered point set has a greater impact on the test results. Hence, how to construct a triangulation more suitable for approximate schemes also needs to be considered in the future work.

Acknowledgment

Supported by the National Natural Science Foundation of China (no. 11271041), National Natural Science Key Foundation of China (no. 10931004) and ISTCP of China grant (no. 2010DFR00700).

References

- [1] W. Xiong, W. Fan, and R. Ding, "Least-squares parameter estimation algorithm for a class of input nonlinear systems," *Journal of Applied Mathematics*, vol. 2012, Article ID 684074, 14 pages, 2012.
- [2] F. Ding, H. Chen, and M. Li, "Multi-innovation least squares identification methods based on the auxiliary model for MISO systems," *Applied Mathematics and Computation*, vol. 187, no. 2, pp. 658–668, 2007.
- [3] F. Ding, P. X. Liu, and G. Liu, "Multi-innovation least-squares identification for system modeling," *IEEE Transactions on Systems, Man, and Cybernetics B*, vol. 40, no. 3, pp. 767–778, 2010.
- [4] R. Z. Feng and R. H. Wang, "Closed smooth surface defined from cubic triangular splines," *Journal of Computational Mathematics*, vol. 23, no. 1, pp. 67–74, 2005.
- [5] R. Z. Feng and R. H. Wang, "Smooth spline surfaces over arbitrary topological triangular meshes," *Journal of Software*, vol. 14, no. 4, pp. 830–837, 2003.
- [6] S. Lee, Ge. Wolberg, and S. Y. Shin, "Scattered data interpolation with multilevel B-splines," *IEEE Transactions on Visualization and Computer Graphics*, vol. 3, no. 3, pp. 228–244, 1997.
- [7] W. Z. Xu, L. T. Guan, and Y. X. Xu, "Smoothing of space scattered data by polynomial natural splines," *Acta Scientiarum Naturalium Universitatis Sunyatseni*, vol. 49, no. 6, pp. 20–30, 2010.
- [8] Z. M. Wu, "Radial basis functions in scattered data interpolation and the meshless method of numerical solution of PDEs," *Chinese Journal of Engineering Mathematics*, vol. 19, no. 2, pp. 1–12, 2002.
- [9] D. Lazzaro and L. B. Montefusco, "Radial basis functions for the multivariate interpolation of large scattered data sets," *Journal of Computational and Applied Mathematics*, vol. 140, no. 1-2, pp. 521–536, 2002.

- [10] R. Feng and L. Xu, "Large scattered data fitting based on radial basis functions," *Computer Aided Drafting, Design and Manufacturing*, vol. 17, no. 1, pp. 66–72, 2007.
- [11] R. Franke and H. Hagen, "Least squares surface approximation using multiquadrics and parametric domain distortion," *Computer Aided Geometric Design*, vol. 16, no. 3, pp. 177–196, 1999.
- [12] T. Sauer and Y. Xu, "On multivariate Hermite interpolation," *Advances in Computational Mathematics*, vol. 4, no. 3, pp. 207–259, 1995.
- [13] Z. M. Wu, "Hermite-Birkhoff interpolation of scattered data by radial basis functions," *Approximation Theory and Its Applications*, vol. 8, no. 2, pp. 1–10, 1992.
- [14] L. Zha and R. Feng, "A scattered hermite interpolation using radial basis Functions," *Journal of Information Computational Science*, vol. 4, pp. 361–369, 2007.
- [15] B. Delaunay, "Sur la sphère vide," *Izvestia Akademii Nauk SSSR, Otdelenie Matematicheskikh i Estestvennykh Nauk*, vol. 7, pp. 793–800, 1934.
- [16] R. Franke and G. Nielson, "Smooth interpolation of large sets of scattered data," *International Journal for Numerical Methods in Engineering*, vol. 15, no. 11, pp. 1691–1704, 1980.
- [17] D. Shepard, "A two-dimensional interpolation function for irregularly spaced data," in *Proceedings of the 23rd ACM National Conference*, pp. 517–524, ACM, 1968.